

SPATIAL MAPPING OF ION DISTRIBUTIONS IN PNEUMATICALLY ASSISTED ELECTROSPRAYS

Patrick Brophy, Thomas McDonald, Jim Murphy
Waters Technologies Corporation, 34 Maple Street, Milford, MA 01757

INTRODUCTION

We investigate the distribution of ions produced from a pneumatically assisted electrospray source under conditions representative of typical liquid chromatography separation under high liquid flow (650 $\mu\text{L min}^{-1}$). Emitter protrusion, angle relative to the MS inlet, ESI voltage, and gas flow are often optimized at the beginning of an MS experiment. Typically, sensitivity towards the response of a single analyte is optimized. Understanding the impact of these parameters on in-source phenomenon (fragmentation, charge state distributions, ion-neutral clustering) and global sensitivity is difficult, if not impossible. The distribution of ions produced in the source have implications for the reproducibility of features observed in non-targeted profiling experiments. Further, these subtle differences can contribute to system-to-system sensitivity variation. The impact of position is investigated here.

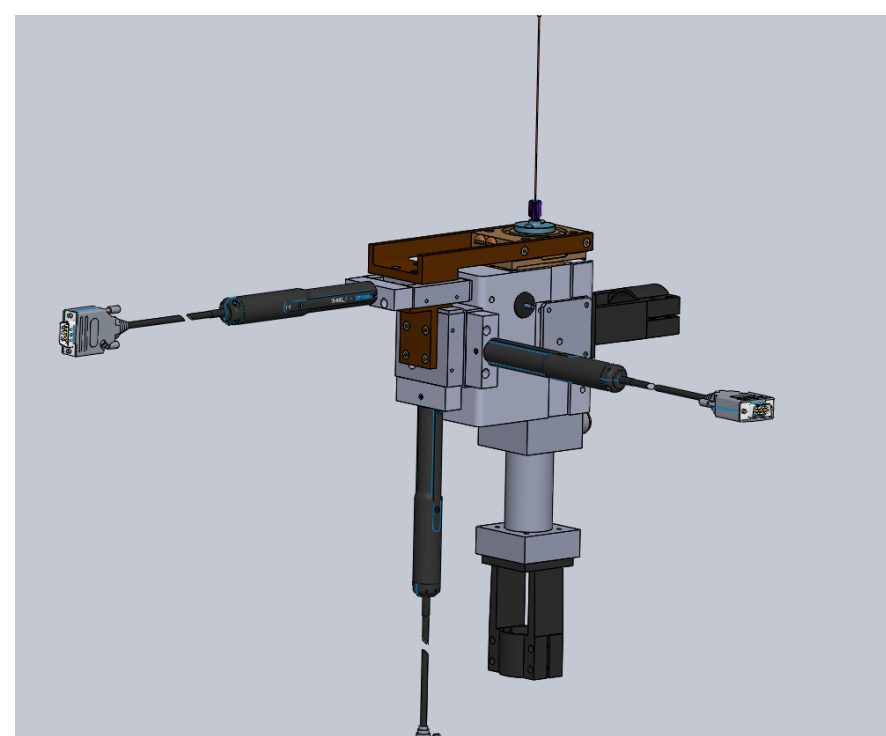


Figure 1. CAD Model of the automated electrospray source used for 3D mapping studies. A: precision stepper motors, B: microscope camera mounts, C: gas inlets, D: liquid emitter, E: exhaust vent

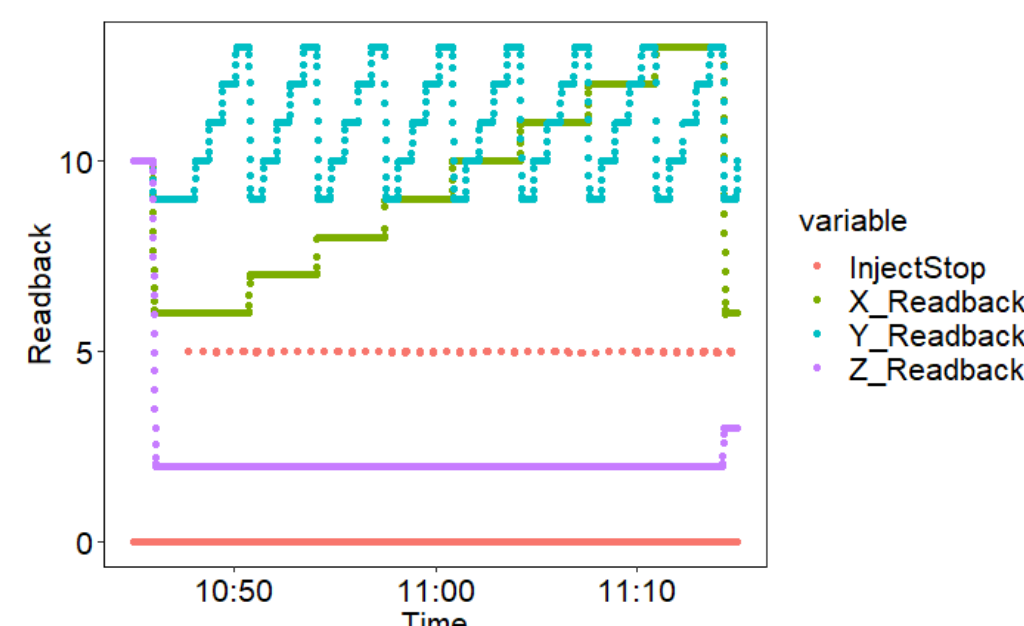


Figure 2. A portion of a single mapping experiment showing movement of stepper motors (X, Y, Z Readbacks) and triggering events (injection Stop).

METHODS

Parameter	Value
ESI Capillary Voltage	800 V
Desolvation Gas Flow	16 L min^{-1}
Nebulizer Gas Flow	1.5 L min^{-1}
Cone Gas Flow	0.35 L min^{-1}
Cone Voltage	5 V (79 V)
Source body temperature	120 °C
Gas heater temperature	600 °C
Stepper Motor Step Size (dx, dy, dz)	1.0 mm
Liquid Flow Rate	650 $\mu\text{L min}^{-1}$
Scan range	50-1000 m/z
Scan rate	1 s
X-travel	-0.365 → 6.135 mm
Y-travel	-1 → 2.5 mm
Z-travel	6.5 → 17 mm

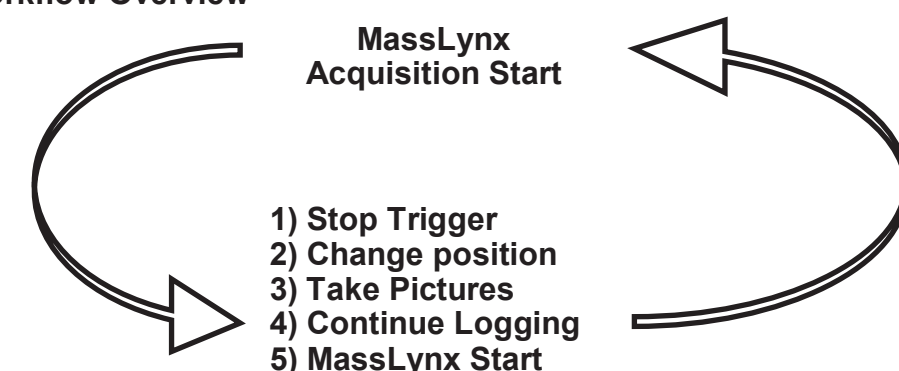
Experimental Setup

A Waters Acquity UPLC I-Class was used to deliver a solution of either leucine enkephalin (0.5 $\mu\text{g mL}^{-1}$) dissolved in 70:30 water:acetonitrile or angiotensin I (1 $\mu\text{g mL}^{-1}$) 80:20 water:acetonitrile at a constant flowrate of 650 $\mu\text{L min}^{-1}$. MassLynx was used to configure the UPLC and MS methods. The coordinate grid and file names were generated in R. A LabVIEW (National Instruments, 2018) program was triggered from the injection start/stop contact closures located on the I-Class back panel via a Labjack U-6 data acquisition device. Each coordinate (x, y, z) investigated consists of a single .raw file where multiple scans are acquired at one or more cone voltages. Gas flows were monitored and controlled with individual mass flow controllers (Alicat Scientific, model MC). Gas temperature was controlled with an Omega process controller (CN132) and 24VDC power supply. Photographs of the emitter and nebulizer were taken from the side and from below the source (Figure 1) using Dino-Lite Digital Microscope Cameras (AM4115ZTW) controlled from LabVIEW using the Dino-Lite SDK. The nebulizer and PEEK mounting block were positioned using stepper motors and controllers (Thorlabs, ZST225B and KST101 Stepper Motor Controller) using the Kinesis .NET controller via LabVIEW.

Data Processing

MSConvert (ProteoWizard) was used to directly convert .raw files to .mzML which were then sequentially loaded into R (Microsoft Open R 3.5.1) using mzR (Bioconductor) and the data.table package for fast data manipulation. Ions of interest ($[\text{M}+\text{H}]^+$, $[\text{M}+\text{Na}]^+$, etc) are extracted within some specified tolerance, averaged across all the scans in the file, and reported for visualization or further processing.

Workflow Overview



RESULTS

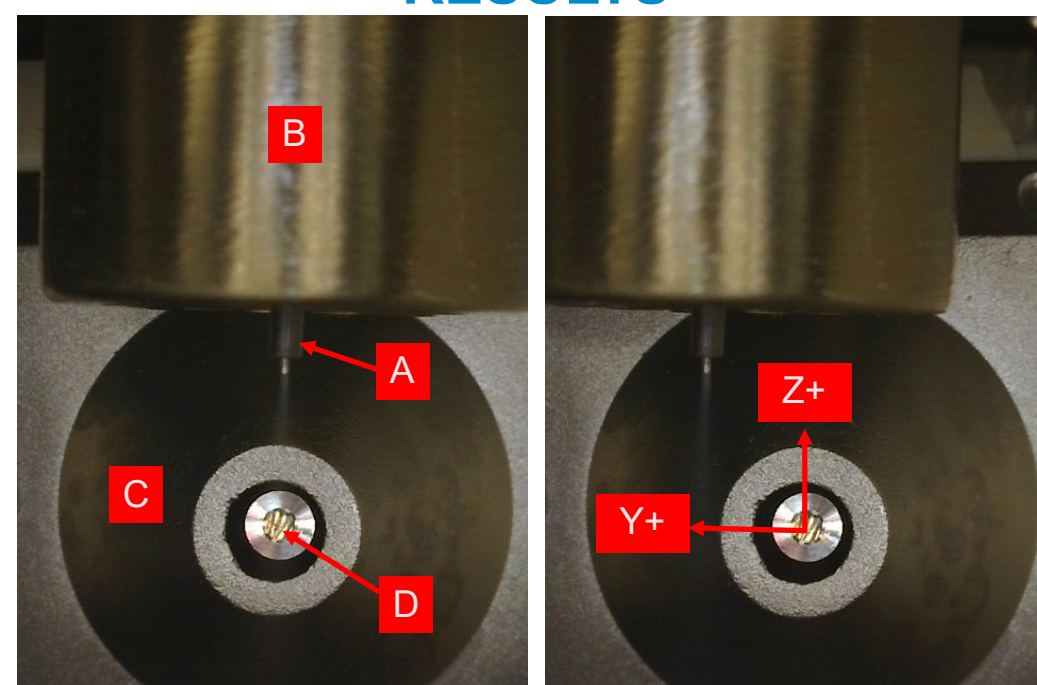


Figure 3. In-source images during electrospray mapping experiment A: showing emitter, B: desolvation gas heater tube, C: gas cone, and D: sample inlet in two different positions.

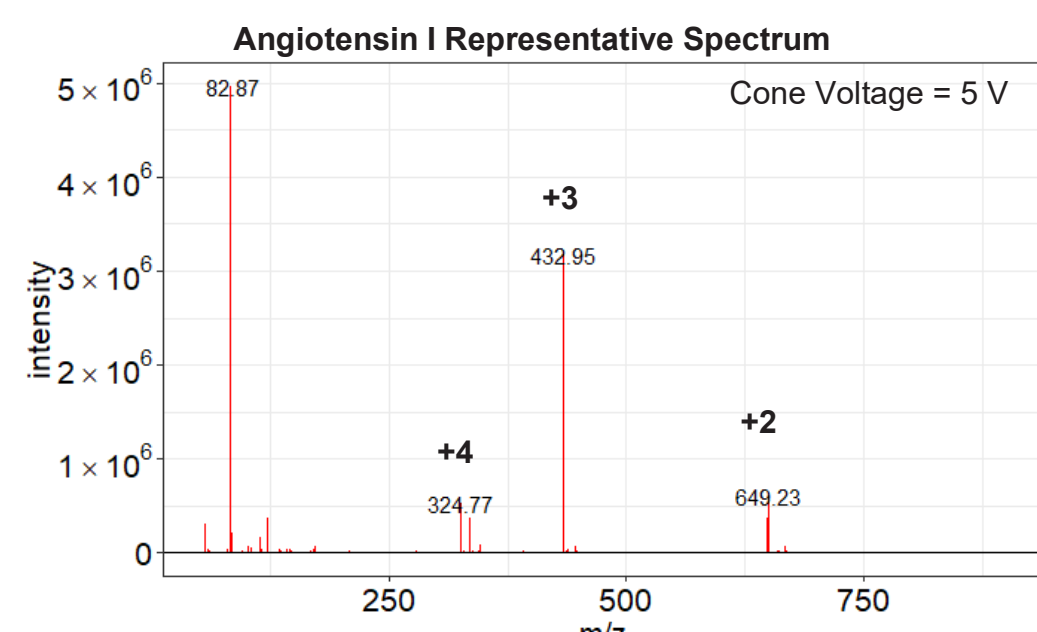


Figure 4. Typical spectrum showing +4, +3 and +2 ions with no evidence of any fragment ions based on theoretical fragment masses.

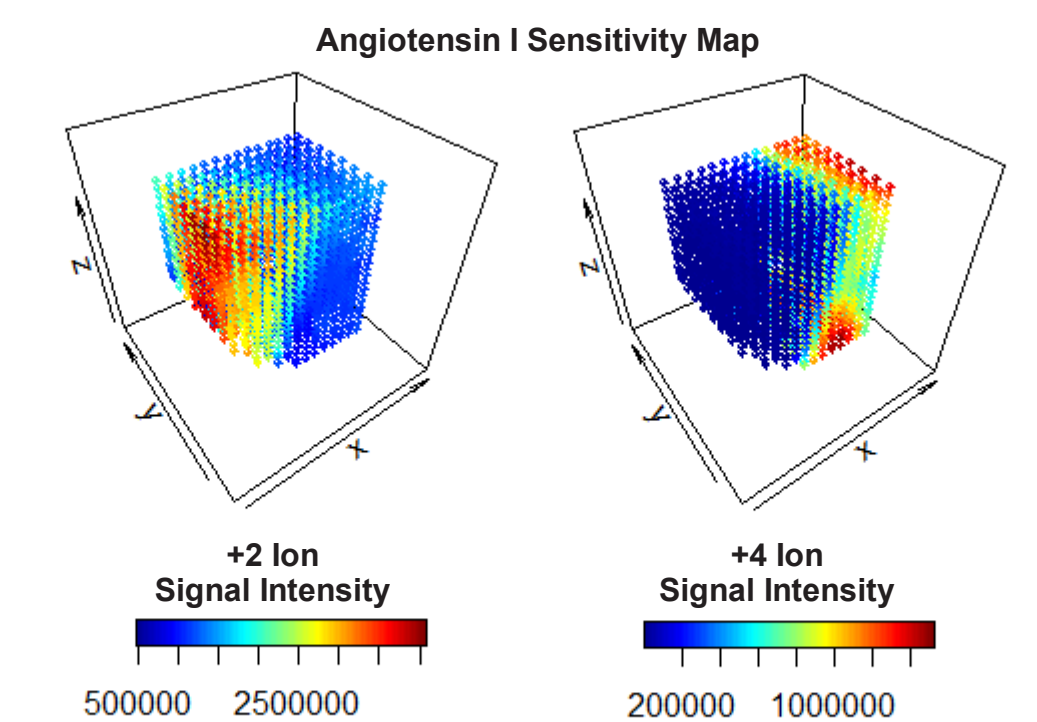


Figure 5. +2 and +4 ion intensity maps for Angiotensin after 3-dimensional interpolation (increase spatial resolution in x, y, z directions by 2x using spline interpolation along x, y, and z independently).

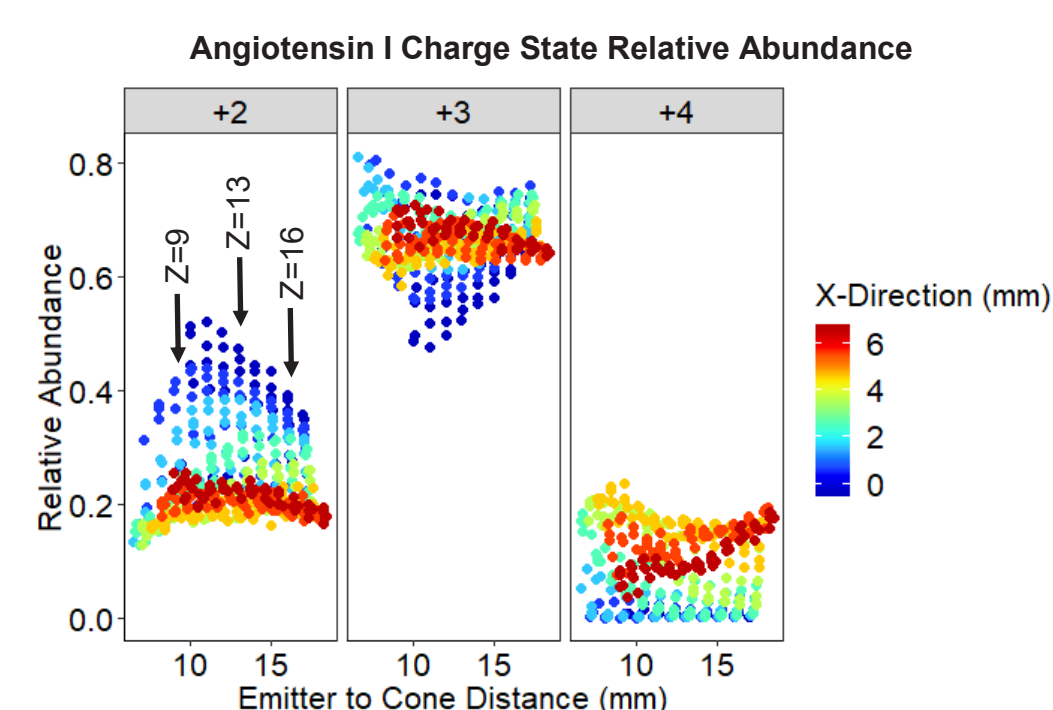


Figure 6. The relative intensity +2, +3, and +4 ions was calculated by dividing the intensity of each individual charge state by the sum of all observed charge states. The points are colored by their distance from the cone in the X-direction showing that at distances sufficiently far from the cone, the charge state distribution remains relatively constant.

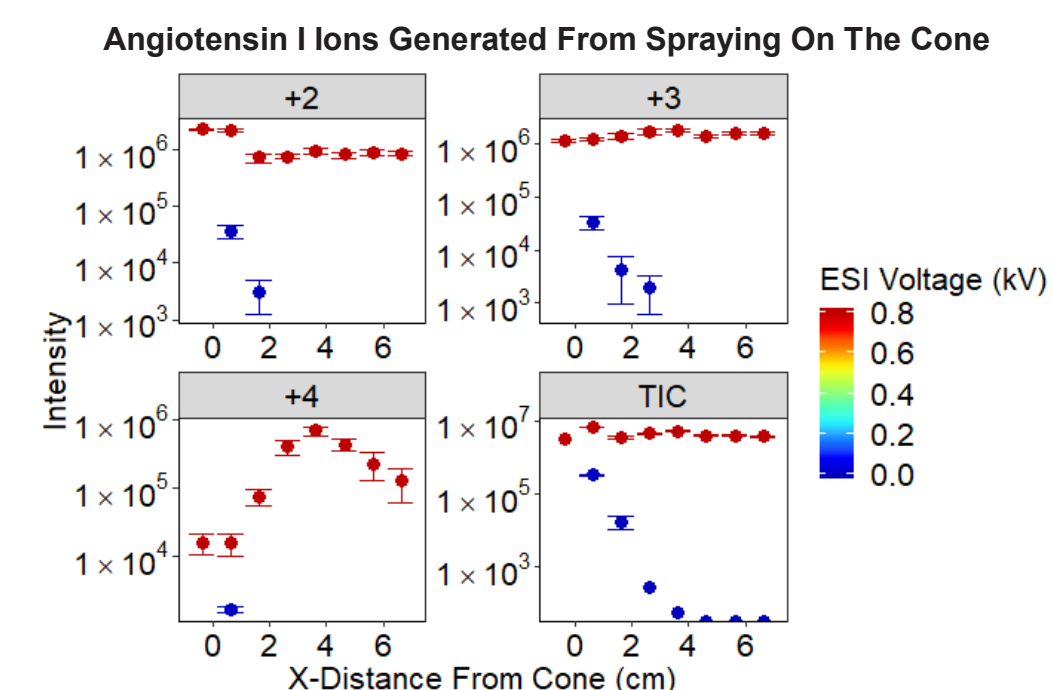


Figure 7. Ions generated from spraying on cone when holding (y, z) = (0,9) and moving along x using nominal ESI voltage

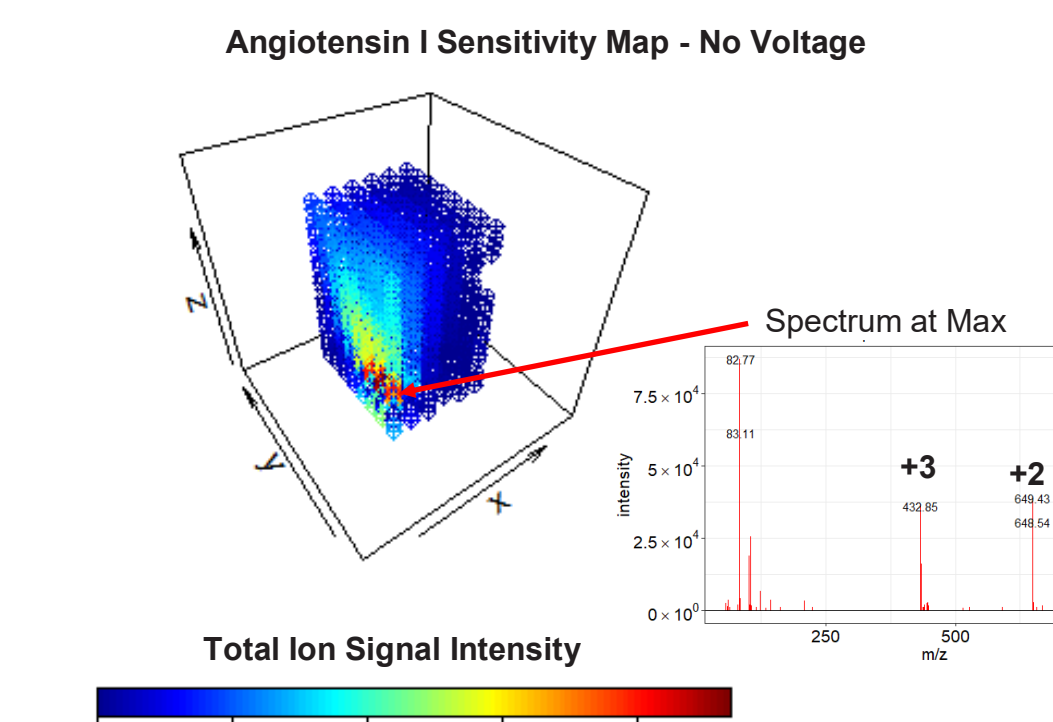


Figure 8. Total ion signal map generated without voltage applied to the emitter.

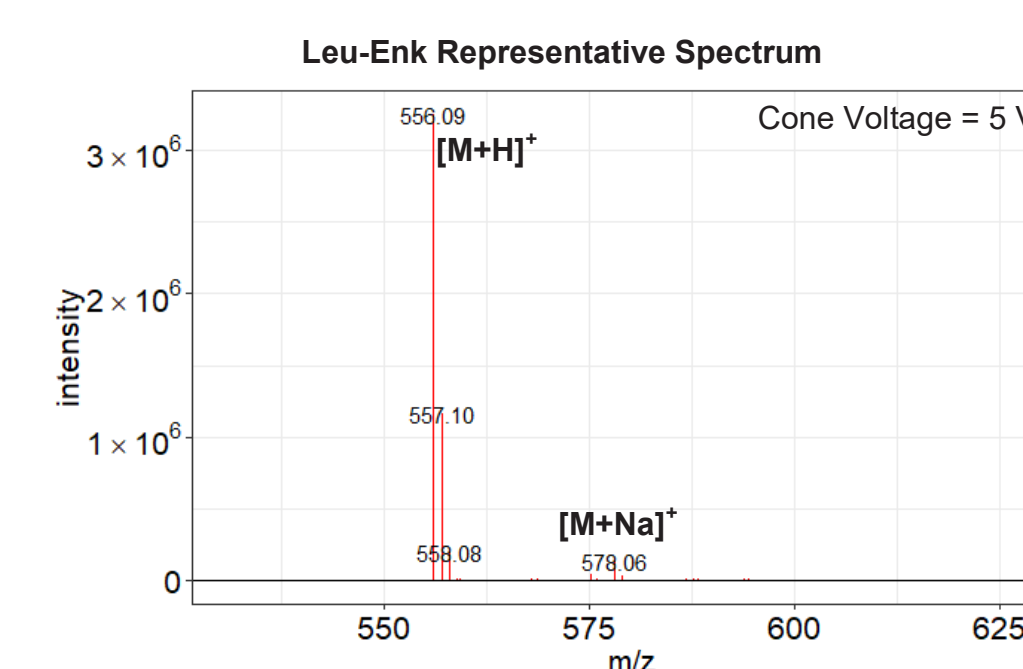


Figure 9. Typical spectrum of Leu-Enk showing $[\text{M}+\text{H}]^+$ and $[\text{M}+\text{Na}]^+$. In-source fragments are not observed with cone voltage set to 5 V.

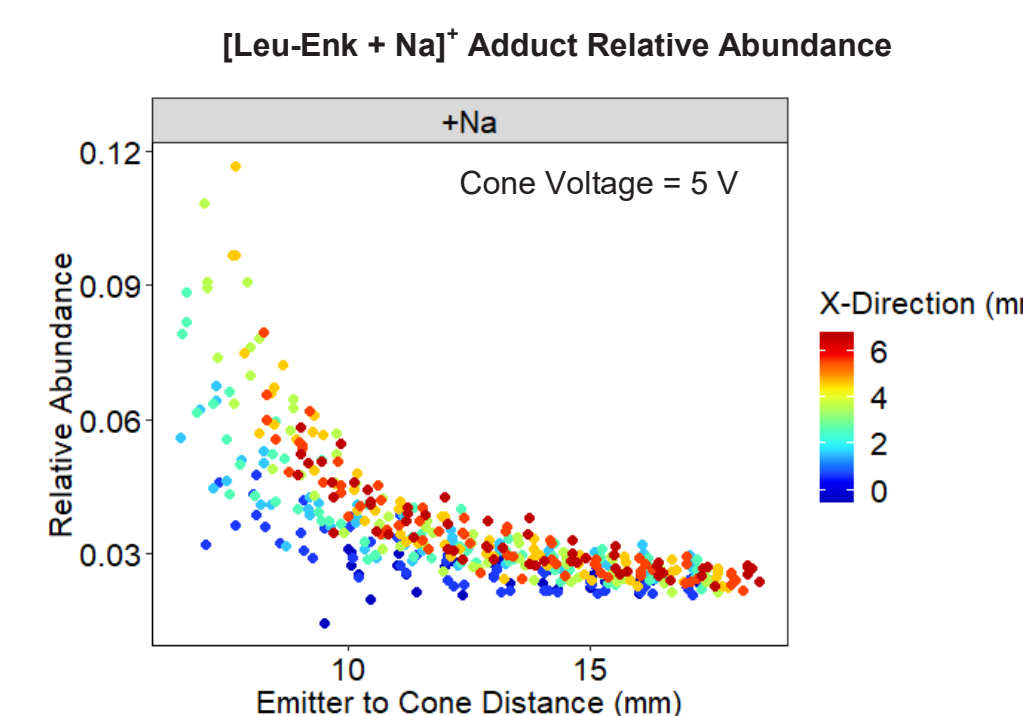


Figure 9. The relative intensity of $[\text{M}+\text{Na}]^+$ was calculated by dividing its intensity by the sum of $[\text{M}+\text{H}]^+$ and $[\text{M}+\text{Na}]^+$. Excursions from the primary trend are less obvious compared to Figure 6 but still present. Points are colored by their distance from the cone in the X-direction.

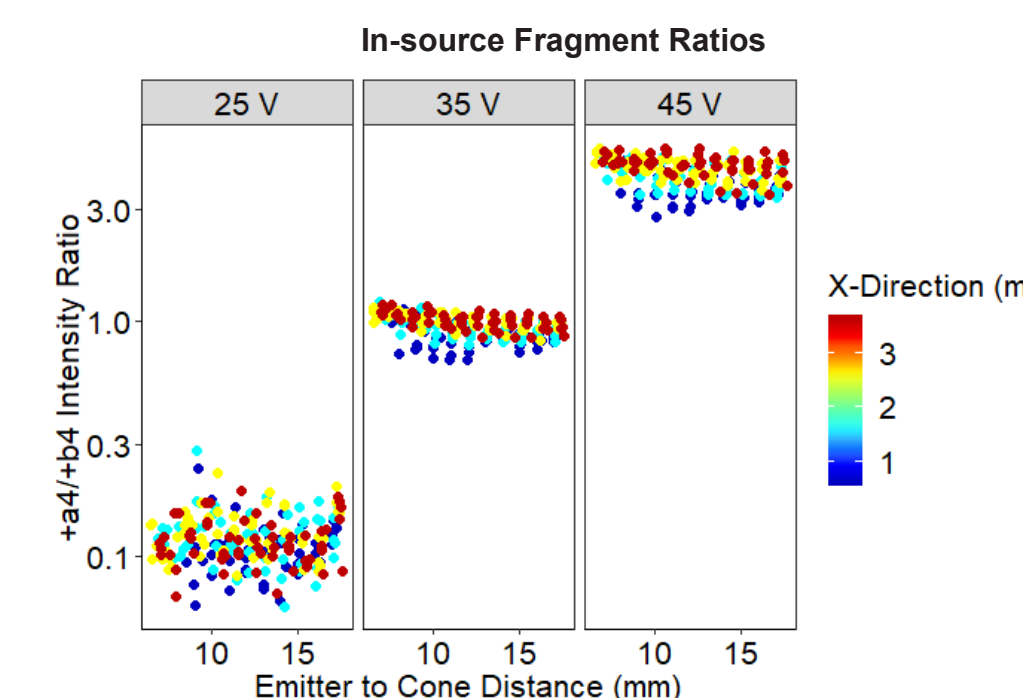


Figure 10. a_4/b_4 ion intensity ratio at cone voltages 25, 35, 45 V (voltages at which fragments are observed).

*Note reduced grid space (x = 0.635 - 3.635).

DISCUSSION

The location at which the maximum sensitivity is achieved depends on the type of the ion being monitored (Figure 5). Total ion signal is maximized when spraying on the cone from the maximum distance from the cone in the Z-direction (not shown). This is likely due to multiple processes including: the generation of ions by impacting droplets on a hot surface (Figure 7), positioning the spray plume directly in-line with the sampling orifice, and increasing the amount of time the ions have to desolvate after nebulization. When examined holistically, the sensitivity to a change in position impacting the ion distribution can be reduced by positioning the emitter at an intermediate distance in the x-direction; this reduces interactions with the cone while maintaining efficient sampling of the spray plume (Figure 6).

Positioning the emitter closer to the inlet reduces the amount of time a droplet has to undergo desolvation, increases the amount of liquid solvent impacting the cone, and increases the electric field strength. $[\text{Leu-Enk} + \text{Na}]^+$ requires more energy to fragment than $[\text{Leu-Enk} + \text{H}]^+$. The increase in the relative abundance of the $[\text{Leu-Enk} + \text{Na}]^+$ appears to be consistent with these processes.

The leu-enk a_4 to b_4 ion abundance ratio has been used previously to characterize ion-energetics¹. Here, this ratio was used to attempt to deconvolute the impact of emitter position ion-formation (adducts, charge states) versus the energy ions experience once being generated. Interestingly, little to no spatial dependence was observed for the a_4 to b_4 abundance ratio. This may suggest the initially produced ion population is more susceptible to changes in emitter positioning than in-source fragments.

These findings are difficult to reconcile in relationship to the other "flavors" of pneumatically assisted (electro)spray. Sonic spray^{2,3}, surface-activated chemical ionization⁴, and the Unispray^{5,6} source commercialized by Waters Corporation all exhibit similarities to the behaviors described here. There likely exist a multitude of processes which contribute to the formation of ions; this work demonstrates that it may be possible to reduce or eliminate the contributions from certain phenomenon in order to improve the stability and reproducibility of an electrospray ion source.

CONCLUSION

Charge State Distributions of Angiotensin I

- If the emitter is positioned to avoid spraying on the gas cone, the charge state distribution is less sensitive to position.
- Components defining the electric field strength are fixed in place leading to improved reproducibility
- Spraying directly on the gas cone produces the largest ion current but produces variable charge state distributions.

Leu-Enk Ion-Neutral Cluster and Fragments

- Behavior is significantly different for the $[\text{M}+\text{Na}]^+$ adduct compared to the multiply charged ions of angiotensin I
- Cone to emitter distance is more important than spraying on the cone
- Maintaining larger distances from the cone reduces variation observed in adduct abundance
- Leu-Enk a_4 to b_4 ratio is insensitive to position

References

1. Thibault, P., Alexander, A. J., Boyd, R. K., Tomer, K. B. Delayed Dissociation Spectra of Survivor Ions from High-Energy Collisional Activation. *J. Am. Soc. Mass Spectrom.*, 1993, 4, 845
2. Hirabayashi, A., Sakurai, M., Takada, Y. Evaporation of Charged Droplets in Atmospheric Pressure Spray Mass Spectrometry. *J. Mass Spectrom. Soc. J.* 1993, 41, 287
3. Hirabayashi, A., Sakurai, M., Koizumi, H. Sonic Spray Ionization Method for Atmospheric Pressure Ionization Mass Spectrometry. *Anal. Chem.* 1994, 66, 4557
4. Cristoni, S., Bernardi, L. R., Blunno, I., Tubaro, M., Guidugli, F. Surface-Activated No-Discharge Atmospheric Pressure Chemical Ionization. *Rapid Commun. Mass Spectrom.* 2003, 17, 1973
5. Bajic, S.: U.S. Patent No. 8,809,777. U.S. Patent and Trademark Office, Washington, DC (2014)
6. Lubin, A., Bajic, S., Cabooter, D., Augustijns, P., Cuyckens, F. Atmospheric Pressure Ionization Using a High Voltage Target Compared to Electrospray Ionization, 2017, 28, 286